

# First Constraints on a Pixelated Universe in Light of DESI

Jonathan J. Heckman,<sup>1,\*</sup> Omar F. Ramadan,<sup>2,†</sup> and Jeremy Sakstein<sup>2,‡</sup>

<sup>1</sup>*Department of Physics and Astronomy, University of Pennsylvania, Philadelphia, PA 19104, USA*

<sup>2</sup>*Department of Physics & Astronomy, University of Hawai'i,  
Watanabe Hall, 2505 Correa Road, Honolulu, HI, 96822, USA*

(Dated: June 2024)

Pixelated dark energy is a string theory scenario with a quantum mechanically stable cosmological constant. The number of pixels that make up the universe slowly increases, manifesting as a time-dependent source of dark energy. DESI has recently reported evidence for dynamical dark energy that fits within this framework. In light of this, we perform the first cosmological analysis of the pixelated model. We find that the simplest model where the pixel growth rate is constant is unable to accommodate the data, providing a comparable fit to  $\Lambda$ CDM; but that models where the pixel growth rate is increasing and of order the Hubble constant today are compatible. Our analysis helps to clarify the features of UV constructions of dark energy necessary to accommodate the data.

## I. INTRODUCTION

The microscopic origin of dark energy remains one of the outstanding issues at the interface of high energy physics and cosmology. While  $\Lambda$ CDM provides an economical framework which accommodates most observational constraints [1], the construction of UV complete models remains an important topic of current research.<sup>1</sup> In addition, recent results from DESI [4] indicate a preference for a dynamic component of dark energy, which has stimulated multiple investigations interpreting the data within the context of competing dark energy models [5–20]. Given this state of affairs, it is natural to seek out UV-motivated dark energy scenarios and investigate which, if any, are favored by data.

In this note we revisit the pixelated dark energy scenario<sup>2</sup> of references [21, 22] which is motivated by top-down string/F-theory considerations. The main idea in this proposal is that at low energies F-theory on a Spin(7) background leads to a 4D model which in Kleinian, i.e., 2 + 2 spacetime signature preserves  $\mathcal{N} = 1/2$  supersymmetry. In Lorentzian, i.e., 3+1 signature this means there is no supersymmetry, but the faint remnant of supersymmetry in Kleinian signature yields states which remain stable against radiative corrections [21–23].

Our interest here is in the potential observational consequences of this proposal in cosmology. The main elements consist of an (unstable) Einstein static Universe of topology  $\mathbb{R} \times S^3$  with a balancing between a stiff fluid ( $w = +1$ ) and dark energy ( $w = -1$ ) which are respectively generated by a three-form flux threading the  $S^3$

and an internal gradient of a dilaton.<sup>3</sup> The presence of fluxes can be viewed as a collection of branes tiling the  $S^3$ , i.e., “pixels” each of which contributes one unit of flux. The unstable nature of the solution leads to a time dependence on the number of pixels, and, consequentially, a time dependent cosmological constant

$$\Lambda(t) = \frac{8\pi^2}{\ell_s^2} \frac{1}{N(t)}, \quad (1)$$

where  $\ell_s$  denotes the string length and the number of pixels  $N(t)$  is time-dependent. From this one obtains a time dependent equation of state (EOS) for dark energy  $P = w\rho$  with [22]:

$$w(t) = -1 + \frac{\dot{N}(t)}{3H(t)N(t)}. \quad (2)$$

Expanding around  $a = 1$ , this fits within the Chevallier-Polarski-Linder (CPL) or  $w_0$ - $w_a$  parameterization of dynamical dark energy [24, 25]:

$$w(a) = w_0 + w_a(1 - a) \text{ with} \quad (3)$$

$$w_0 = -1 + \frac{\dot{N}}{3H_0 N} \text{ and} \quad (4)$$

$$w_a = -\frac{1}{2}\Omega_{m,0} \frac{\dot{N}}{H_0 N}. \quad (5)$$

In the regime of interest, i.e., close to present day values,  $\dot{N} > 0$  so  $w_0 > -1$  and  $w_a < 0$ . The quantity  $\dot{N}/N = \Gamma$  is the growth rate/decay rate of the pixels (depending on the sign of the derivative). In deriving equations (4) and (5) it was assumed that  $\Gamma$  is approximately constant i.e.,  $\dot{\Gamma}/\Gamma \ll H$  and that  $\Gamma/H_0 \ll 1$  so that higher-order

\* [jheckman@sas.upenn.edu](mailto:jheckman@sas.upenn.edu)

† [oramadan@hawaii.edu](mailto:oramadan@hawaii.edu)

‡ [sakstein@hawaii.edu](mailto:sakstein@hawaii.edu)

<sup>1</sup> For recent reviews of the rather large literature, see e.g., [2, 3] and references therein.

<sup>2</sup> We refer to this as a scenario since a complete top-down implementation of the proposal remains to be carried out.

<sup>3</sup> We note that, while the model has positive spatial curvature, the requirements that inflation is reproduced implies that  $\Omega_\kappa$  is far smaller than the observational bounds [22] so for all intents and purposes the universe is flat. We will therefore neglect spatial curvature in what follows.

terms may be neglected [22]. While this is the simplest choice, it is generically expected that  $\Gamma$  is time-dependent so we shall revisit this possibility later. We derive equations (3)–(5) in Appendix A where we also use our results to confirm that when  $\Gamma$  is assumed to be constant the approximation  $\Gamma/H_0 \ll 1$  is valid *a posteriori*. Equations (4) and (5) imply the relation

$$1 + w_0 = -\frac{2}{3\Omega_{m,0}} w_a, \quad (6)$$

implying that pixelated dark energy with constant  $\Gamma$  has one fewer parameter than  $w_0$ - $w_a$ ; the theory is a one-parameter extension of  $\Lambda$ CDM. We now test the pixelated DE model against cosmological observations for the first time. Turning the discussion around, we can also use our best fit to extract a data driven estimate of  $\Gamma = \dot{N}/N$ , the growth rate of pixels in this model.

## II. METHOD AND RESULTS

We modified the cosmological solver CLASS [26, 27] to evolve the cosmology of pixelated DE according to equation (3) with the relation (6). For the standard  $w_0$ - $w_a$  parameterization, we sampled over the 6  $\Lambda$ CDM parameters  $\{A_s, n_s, 100\theta_*, \Omega_b h^2, \Omega_c h^2, \tau_{reio}\}$  plus  $\{w_0, w_a\}$ . However, for pixelated DE, equation (6) implies that  $w_a$  is a derived parameter given by a combination of the sampled  $\Omega_{m,0}$  and  $w_0$ , so we only sampled over  $\{A_s, n_s, 100\theta_*, \Omega_b h^2, \Omega_c h^2, \tau_{reio}, w_0\}$ . We fitted both models to the combination of cosmic microwave background (CMB) data, specifically the Planck 2018 CMB spectra [1], CMB gravitational lensing from a combination of Planck 2020 lensing [28, 29] and ACT DR6 [30, 31]; the DESI BAO measurements [4]; and the Union3 [32] supernovae compilation. This combination of data is identical to that used by the DESI analysis [33]. The Markov Chain Monte Carlo (MCMC) sampling was performed using the Cobaya code [34]; the sampler was deemed to have converged when the standard Gelman-Rubin criteria  $R-1 < 0.01$  [35] was achieved. For pixelated DE, we imposed the priors  $w_0 \sim \mathcal{U}[-1, 1]$ , which reflect the requirement in Eq. (3) that  $w(a) \geq -1$  in pixelated DE, while for the  $w_0$ - $w_a$  parameterization we imposed a wide prior with  $w_0 \sim \mathcal{U}[-3, 1]$  and  $w_a \sim \mathcal{U}[-3, 2]$ . We analyzed and plotted our chains using GetDist [36]. For comparative purposes, we also fitted a general CPL  $w_0$ - $w_a$  model. Our results are given in table I, with 2D contour plots and 1D marginalized posteriors given in figure 2.

For the general CPL model, we find consistent results with DESI [4]:  $w_0 = -0.66 \pm 0.10$ ,  $w_a = -1.22^{+0.42}_{-0.33}$  and confirm their findings that this model is preferred over  $\Lambda$ CDM at the  $\sim 3\sigma$  level. The pixelated DE relation yielded  $w_0 < -0.949$  and  $w_a = -0.0192^{+0.019}_{-0.0083}$ . We derived the pixel growth rate with its 68% confidence

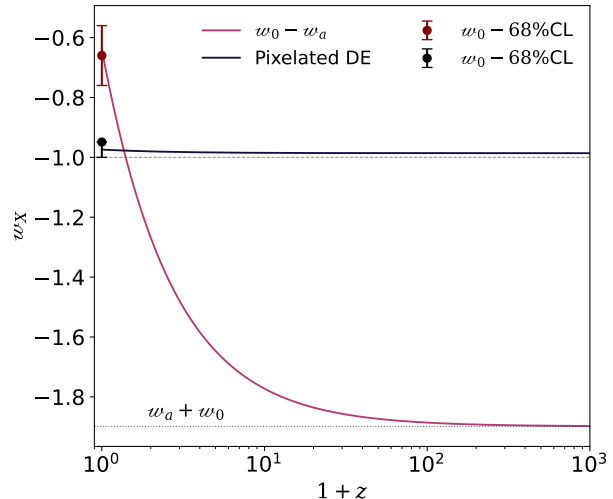


Figure 1. The best fitting EOS for the  $w_0 w_a$ CDM model and pixelated dark energy. The CPL parameterization suggests that the dark energy fluid initially has an equation of state of  $w_a + w_0 = -1.9$ , represented by the dotted line, for  $z \gtrsim 10^3$ . The EOS evolves around redshift  $z \approx 10^3$ , crossing the phantom line  $w = -1$  at  $z \approx 0.4$ , coinciding with the onset of dark energy domination. The black solid line is the EoS of pixels in which the field starts frozen at  $w = -0.986$  and evolves to  $w_0 = -0.974$  today. The dashed line represents the EOS for a cosmological constant,  $w_\Lambda = -1$ . We also show the 68% confidence level posteriors of  $w_0$  for both  $w_0 w_a$ CDM and pixelated DE in red and black, respectively.

interval:

$$\frac{\Gamma}{H_0} = 0.121^{+0.060}_{-0.12} \quad (7)$$

with the best fitting value  $(\Gamma/H_0)_{\text{best fit}} = 0.078$ , indicating that the number of pixels is increasing at a smaller rate than the expansion of the universe.

The data showed no significant preference for the model over  $\Lambda$ CDM. In fact, we find that the posteriors of our model are well within  $1\sigma$  of the  $\Lambda$ CDM posteriors for the six  $\Lambda$ CDM parameters, with  $w_0$  and  $w_a$  being within  $2\sigma$ . Moreover, with one extra parameter, we found a negligible improvement of  $\Delta\chi^2_{\text{best fit}} = -1.68$ . The statistical expectation is that we expect, minimally, an improvement of fit by  $\Delta\chi^2_{\text{best fit}} = -1$  for one additional parameter. Since DESI and Union3 prefer a dynamical DE at low redshifts, and that only the posteriors of  $w_0$  and  $w_a$  are  $> 1\sigma$  from  $\Lambda$ CDM, we interpret this extra  $\Delta\chi^2_{\text{best fit}} \approx -0.68$  as a negligible preference for pixelated DE over  $\Lambda$ CDM for having  $w(z) > -1$  at low redshifts. The small improvement suggests that the additional complexity of our model does not significantly enhance the fit compared to the simpler  $\Lambda$ CDM, yet it is in the correct direction.

Despite predicting the CPL parameterization of DE, pixelated DE with constant  $\Gamma$  is unable to provide a

Parameter & Model	Flat $\Lambda$ CDM	$w_a w_a$ CDM	Pixelated Dark Energy
<b>Sampled Parameters</b>			
$\log(10^{10} A_s)$	$3.053(3.059)_{-0.014}^{+0.013}$	$3.040(3.040) \pm 0.013$	$3.057(3.057)_{-0.016}^{+0.013}$
$n_s$	$0.9681(0.9688) \pm 0.0036$	$0.9657(0.9668) \pm 0.0038$	$0.9693(0.9699) \pm 0.0038$
$\Omega_b h^2$	$0.02245(0.02247) \pm 0.00013$	$0.02238(0.02242) \pm 0.00014$	$0.02249(0.02251) \pm 0.00014$
$\Omega_c h^2$	$0.11876(0.11856) \pm 0.00084$	$0.11969(0.11982) \pm 0.00096$	$0.11834(0.11834) \pm 0.00090$
$100\theta_*$	$1.04199(1.041931) \pm 0.00028$	$1.04187(1.04185) \pm 0.00029$	$1.04202(1.04200) \pm 0.00029$
$\tau_{\text{reio}}$	$0.0590(0.0614) \pm 0.0071$	$0.0526(0.0529) \pm 0.0072$	$0.0612(0.0618) \pm 0.0074$
$w_0$	...	$-0.66(-0.68) \pm 0.10$	$< -0.949(-0.974)$
$w_a$	...	$-1.22(-1.14)_{-0.33}^{+0.42}$	$-0.0192(-0.0121)_{-0.0083}^{+0.019}$
<b>Derived Parameters</b>			
$H_0$ [km/s/Mpc]	$67.92(67.98) \pm 0.38$	$66.51(66.61) \pm 0.95$	$67.05(67.44)_{-0.71}^{+0.81}$
$\Omega_m$	$0.3075(0.3065) \pm 0.0050$	$0.3228(0.3221) \pm 0.0095$	$0.3148(0.3111)_{-0.0083}^{+0.0073}$
<b><math>\chi^2</math> Statistics</b>			
$\chi_{\text{bf}}^2(\Delta)$	2835.45	2822.10(-13.5)	2833.77(-1.68)
$\chi_{\text{bf}}^2/\text{DoF}$	1.21	1.21	1.21
Tension Level	...	$3.02\sigma$	...

Table I. Marginalized posteriors for flat  $\Lambda$ CDM,  $w_0 w_a$ CDM, and pixelated DE models using CMB+DESI+Union3 likelihoods, showing the mean(best fit) and the 68% confidence interval. The  $\Lambda$ CDM parameters share the same prior across models and only the priors of  $\{w_0, w_a\}$  parameters differ in  $w_0 w_a$ CDM and pixelated DE. We also show the best fitting  $\chi_{\text{bf}}^2(\Delta)$ , where  $\Delta = \chi_{\text{bf,model}}^2 - \chi_{\text{bf},\Lambda\text{CDM}}^2$  is the difference between the best fitting  $\chi^2$  values, subtracted from that of  $\Lambda$ CDM. The statistically significant tension levels with  $\Lambda$ CDM are reported as well.

good fit to the data. The reason for this is that the relation between  $w_0$  and  $w_a$  in equation (6) does not allow  $w(z)$  to vary rapidly enough to provide a good fit to the data at all redshifts. To elaborate, the supernovae and DESI data at redshift  $z \lesssim 0.51$  deviates from the  $\Lambda$ CDM prediction while higher redshift DESI data is consistent (see [4–7, 11] for additional discussion on this). The CPL model is able to fit the data at all redshifts by having  $w_0 > -1$  and  $w_a$  negative and large in magnitude, with  $w_a \sim 2w_0$  so that  $w(z)$  approaches  $-1$  rapidly when  $z > 0.51$ . On the other hand, the  $w_0$ - $w_a$  model corresponding to pixelated DE does not allow for this. As demonstrated by equations (4) and (5),  $w_0$  differs from  $-1$  by an amount of order  $\Gamma/H_0$  so fitting the low- $z$  data requires  $\Gamma/H_0 \sim \mathcal{O}(10^{-1})$  implying that  $w_a \sim \mathcal{O}(10^{-2})$  because it is suppressed by a factor of  $\Omega_{m,0} \sim 0.3$  relative to  $\Gamma/H_0$ . Thus, the EOS evolves negligibly over the range of relevant redshifts so the model is unable to accommodate all of the data. This is exemplified in figure 1 where we plot the best fitting CPL and pixelated DE equation of state as a function of redshift. At  $z > 0$  the CPL model EOS rapidly moves from  $w > -1$  towards  $w = -1$  but the pixelated DE EOS barely evolves.

### III. OUTLOOK

The considerations above provide guidance for constructing UV complete models of dark energy that are able to accommodate the data. Clearly, breaking the relation between  $w_0$  and  $w_a$  that forces  $|w_a| < w_0$  is necessary. This can be accomplished by moving beyond the approximation that the pixel growth rate  $\Gamma$  is constant. We derive the CPL parameterization for this more general case in Appendix A for the first time. We find

$$w_0 = -1 + \frac{\Gamma_0}{3H_0} \text{ and} \quad (8)$$

$$w_a = -\frac{1}{2}\Omega_{m,0} \frac{\Gamma_0}{H_0} - \frac{\Gamma_1}{3H_0^2} - (1 - \Omega_{m,0}) \frac{\Gamma_0^2}{6H_0^2}, \quad (9)$$

where:

$$\Gamma_0 = \left. \frac{\dot{N}}{N} \right|_0 \quad \text{and} \quad \Gamma_1 = \left. \frac{\ddot{N}}{N^2} \right|_0 - \Gamma_0^2, \quad (10)$$

with subscript zeros indicating quantities evaluated at the present time  $t_0$ . Thus, in the general case, the equation of state also depends on  $\dot{N}/N^2$ .

This gives a less restricted two-parameter model that can be fit to the data to bound  $\Gamma_0$  and  $\Gamma_1$ . The CPL

bounds cannot be directly translated into bounds on  $\Gamma_0$  and  $\Gamma_1$  because, in the pixelated model,  $w_a$  depends on  $\Omega_{m,0}$ , which is simultaneously varied in the MCMC so a full fit to the data is required to account for this. We can however estimate  $\{\Gamma_0, \Gamma_1\}$  by using the best-fitting parameters in our  $w_0 w_a$ CDM analysis. Doing so, we estimated the 68% confidence interval

$$\frac{\Gamma_0}{H_0} = 1.03 \pm 0.30 \quad \text{and} \quad \frac{\Gamma_1}{H_0^2} = 2.77 \pm 0.80, \quad (11)$$

with the best fitting values  $(\Gamma_0/H_0)_{\text{best fit}} = 0.96$  and  $(\Gamma_1/H_0^2)_{\text{best fit}} = 2.63$ . In terms of the pixel number acceleration, we found the 68% CL

$$\frac{\ddot{N}}{N^2 H_0^2} = 3.9^{+1.1}_{-1.6} \quad (12)$$

with best fitting value  $[\ddot{N}/(NH_0)^2]_{\text{best fit}} = 3.56$ . Thus, the data indicate that the pixel growth rate today is comparable with the expansion rate of the universe, and is beginning to increase. Deriving the full time-dependence of the pixel decay rate in the UV-construction and determining whether this scenario can be realized is then paramount.<sup>4</sup> Turning the discussion around, a detailed fit with the extra parameter  $\Gamma_1$  would provide important hints on the microphysical dynamics of pixels.

## ACKNOWLEDGMENTS

We are grateful for discussions with Jason Kumar, Craig Lawrie, David Rubin, Greg Tarlé, and Xerxes Tata. The technical support and advanced computing resources from University of Hawai‘i Information Technology Services – Cyberinfrastructure, funded in part by the National Science Foundation CC awards #2201428 and #2232862 are gratefully acknowledged. The work of JJH is supported by DOE (HEP) Award DE-SC0013528.

## Appendix A: CPL Parameterization For Pixelated Dark Energy

In this Appendix, we derive equations (8) and (9), which have not previously appeared in the literature. Our starting point is the EOS for pixelated DE derived by [22] given in equation (2). The late-time universe is well-approximated as consisting of matter and a time-dependent cosmological constant given by  $\Lambda(t) = \Lambda_0/N(t)$  with  $\Lambda_0 = 8\pi^2/l_s^2$  (see equation (1)) so the Friedmann equation is

$$H^2(t) = \frac{\Omega_{m,0} H_0^2}{a(t)^3} + \frac{H_0^2(1 - \Omega_{m,0})N_0}{N(t)}, \quad (A1)$$

where  $N_0 = N(t_0)$  is the number of pixels at the present time, and  $\Lambda_0$  has been replaced by  $N_0$  using the relation  $\Lambda_0 = 3H_0^2 N_0(1 - \Omega_{m,0})$ . One can then Taylor expand Eq. (A1) to first-order in  $(1 - a)$ , similarly expand  $\Gamma(t)$ , and substitute both into equation (2) to find the CPL parameterization with  $w_0$  and  $w_a$  given in equations (8) and (9) with  $\{\Gamma_0, \Gamma_1\}$  given in Eq. (10).

In the constant  $\Gamma_0$  analysis above, we made the approximation that  $\Gamma_0/H_0 \ll 1$ . We now verify that this was justified. The best fitting model gave  $\Gamma_0/H_0 = 0.078$  so the error in  $w_a$  by neglecting the final two terms in Eq. (9) is  $\Delta w_a = 2.7 \times 10^{-3}$ , an order of magnitude smaller than both the best fitting value of  $w_a$  and its error bars.

<sup>4</sup> As an example, [22] also found there can be larger jumps in the number of pixels from thermal and quantum events, leading to an acceleration in the pixel number.

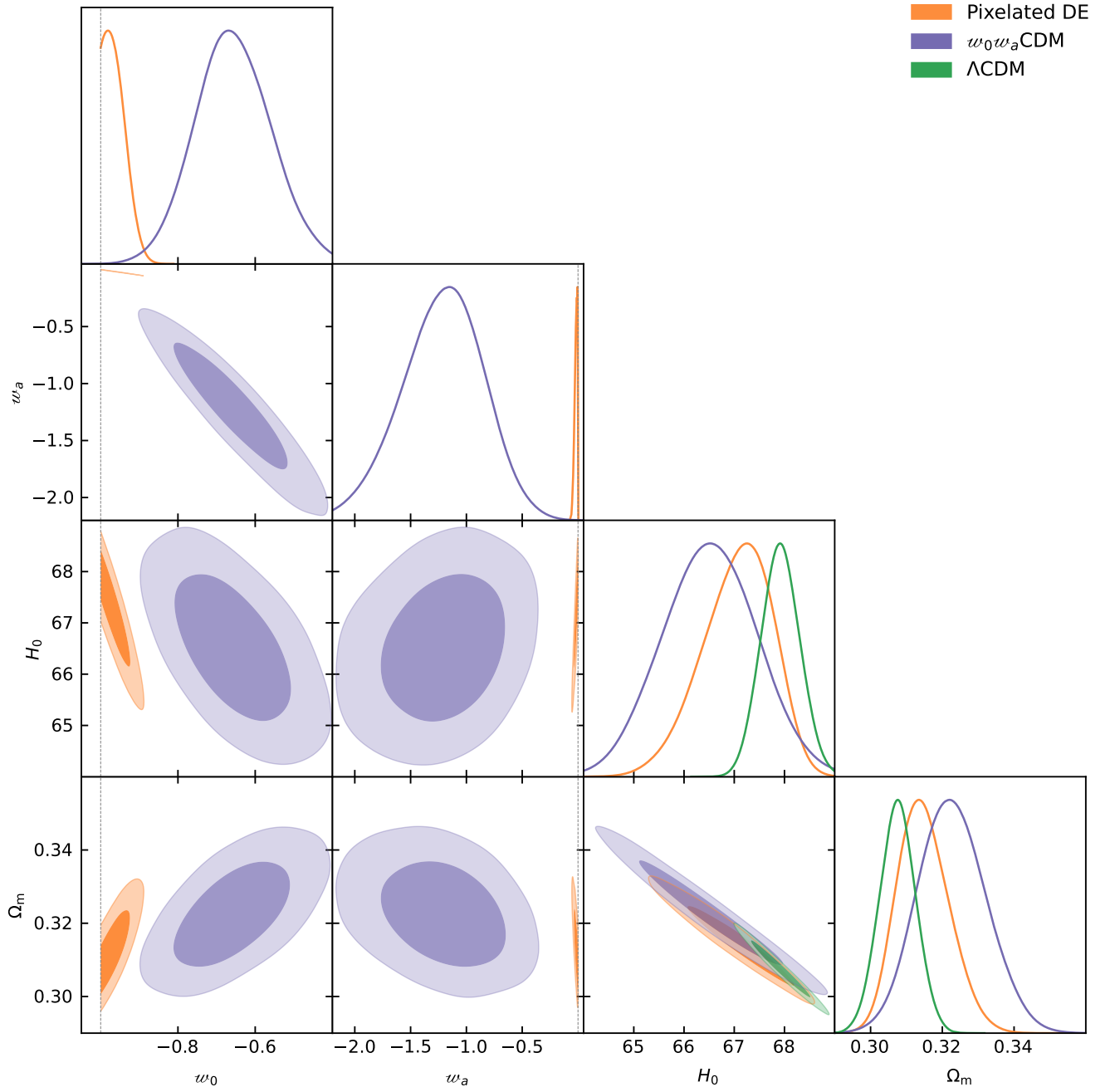


Figure 2. Marginalized posteriors for different cosmologies fitted to CMB+DESI+Union3. The inner contours represent the 68% confidence level (CL) where the outer is 95% CL. The dashed lines indicate the  $\Lambda$ CDM limit with  $w_0 = -1$  and  $w_a = 0$ . Both  $w_0w_a$ CDM and pixelated DE include the  $\Lambda$ CDM limit, with pixelated DE converging to  $\Lambda$ CDM within 68% confidence interval.

- 
- [1] N. Aghanim *et al.* (Planck), *Astron. Astrophys.* **641**, A6 (2020), [Erratum: *Astron. Astrophys.* 652, C4 (2021)], [arXiv:1807.06209 \[astro-ph.CO\]](#).
- [2] M. Cicoli, J. P. Conlon, A. Maharana, S. Parameswaran, F. Quevedo, and I. Zavala, *Phys. Rept.* **1059**, 1 (2024), [arXiv:2303.04819 \[hep-th\]](#).
- [3] T. Van Riet and G. Zoccarato, *Phys. Rept.* **1049**, 1 (2024), [arXiv:2305.01722 \[hep-th\]](#).
- [4] A. G. Adame *et al.* (DESI), (2024), [arXiv:2404.03002 \[astro-ph.CO\]](#).
- [5] E. O. Colgáin, M. G. Dainotti, S. Capozziello, S. Pourojaghi, M. M. Sheikh-Jabbari, and D. Stojkovic, (2024), [arXiv:2404.08633 \[astro-ph.CO\]](#).
- [6] O. F. Ramadan, J. Sakstein, and D. Rubin, (2024), [arXiv:2405.18747 \[astro-ph.CO\]](#).
- [7] S. Bhattacharya, G. Borghetto, A. Malhotra, S. Parameswaran, G. Tasinato, and I. Zavala, (2024), [arXiv:2405.17396 \[astro-ph.CO\]](#).
- [8] Y. Carloni, O. Luongo, and M. Muccino, (2024), [arXiv:2404.12068 \[astro-ph.CO\]](#).
- [9] C.-G. Park, J. de Cruz Perez, and B. Ratra, (2024), [arXiv:2405.00502 \[astro-ph.CO\]](#).
- [10] M. Cortês and A. R. Liddle, (2024), [arXiv:2404.08056 \[astro-ph.CO\]](#).
- [11] D. Shlivko and P. Steinhardt, (2024), [arXiv:2405.03933 \[astro-ph.CO\]](#).
- [12] B. R. Dinda, (2024), [arXiv:2405.06618 \[astro-ph.CO\]](#).
- [13] D. Wang, (2024), [arXiv:2404.06796 \[astro-ph.CO\]](#).
- [14] O. Luongo and M. Muccino, (2024), [arXiv:2404.07070 \[astro-ph.CO\]](#).
- [15] H. Wang and Y.-S. Piao, (2024), [arXiv:2404.18579 \[astro-ph.CO\]](#).
- [16] Y. Tada and T. Terada, (2024), [arXiv:2404.05722 \[astro-ph.CO\]](#).
- [17] W. Yin, *JHEP* **05**, 327 (2024), [arXiv:2404.06444 \[hep-ph\]](#).
- [18] K. V. Berghaus, J. A. Kable, and V. Miranda, (2024), [arXiv:2404.14341 \[astro-ph.CO\]](#).
- [19] D. Andriot, S. Parameswaran, D. Tsimpis, T. Wrase, and I. Zavala, (2024), [arXiv:2405.09323 \[hep-th\]](#).
- [20] Y. Yang, X. Ren, Q. Wang, Z. Lu, D. Zhang, Y.-F. Cai, and E. N. Saridakis, (2024), [arXiv:2404.19437 \[astro-ph.CO\]](#).
- [21] J. J. Heckman, C. Lawrie, L. Lin, and G. Zoccarato, *Fortsch. Phys.* **67**, 1900057 (2019), [arXiv:1811.01959 \[hep-th\]](#).
- [22] J. J. Heckman, C. Lawrie, L. Lin, J. Sakstein, and G. Zoccarato, *Fortsch. Phys.* **67**, 1900071 (2019), [arXiv:1901.10489 \[hep-th\]](#).
- [23] J. J. Heckman, A. Joyce, J. Sakstein, and M. Trodden, *Int. J. Mod. Phys. A* **37**, 2250201 (2022), [arXiv:2208.02267 \[hep-th\]](#).
- [24] M. Chevallier and D. Polarski, *Int. J. Mod. Phys. D* **10**, 213 (2001), [arXiv:gr-qc/0009008](#).
- [25] E. V. Linder, *Phys. Rev. Lett.* **90**, 091301 (2003), [arXiv:astro-ph/0208512](#).
- [26] D. Blas, J. Lesgourgues, and T. Tram, *JCAP* **07**, 034 (2011), [arXiv:1104.2933 \[astro-ph.CO\]](#).
- [27] J. Lesgourgues, (2011), [arXiv:1104.2932](#).
- [28] Y. Akrami *et al.* (Planck), *Astron. Astrophys.* **643**, A42 (2020), [arXiv:2007.04997 \[astro-ph.CO\]](#).
- [29] J. Carron, M. Mirmelstein, and A. Lewis, *JCAP* **09**, 039 (2022), [arXiv:2206.07773 \[astro-ph.CO\]](#).
- [30] F. J. Qu *et al.* (ACT), *Astrophys. J.* **962**, 112 (2024), [arXiv:2304.05202 \[astro-ph.CO\]](#).
- [31] M. S. Madhavacheril *et al.* (ACT), *Astrophys. J.* **962**, 113 (2024), [arXiv:2304.05203 \[astro-ph.CO\]](#).
- [32] D. Rubin *et al.*, (2023), [arXiv:2311.12098 \[astro-ph.CO\]](#).
- [33] T. M. C. Abbott *et al.* (DES), (2024), [arXiv:2401.02929 \[astro-ph.CO\]](#).
- [34] J. Torrado and A. Lewis, *JCAP* **05**, 057 (2021), [arXiv:2005.05290](#).
- [35] A. Gelman and D. B. Rubin, *Statist. Sci.* **7**, 457 (1992).
- [36] A. Lewis, (2019), [arXiv:1910.13970 \[astro-ph.IM\]](#).